Interaction Surfaces for Post-Fire Analysis Based on Minkowski Sum

Milan Bursać[1*], Saša Stošić[1]

[1]Faculty of Civil Engineering, Belgrade, Serbia

Paper type: Original scientific paper
Received: 21.2.2023.
Accepted: 12.5.2023.
Published: 30.9.2023.

UDK: 614.84
DOI: 10.14415/JFCE-889

Abstract:

The primary aims of this paper are twofold: firstly, to employ Minkowski sum to assess the interaction surfaces of a reinforced concrete section in a post-fire analysis, and secondly, to investigate the impact of fire length on load-bearing capacity for a simple example of a beam under four-point bending. The approach used in this study has previously been utilized for fire scenarios and can be easily adapted for post-fire analysis purposes. The Minkowski sum method is utilized to generate interaction surfaces by combining multiple basic geometric shapes into a more intricate shape. In this case, the simpler shapes used are ellipsoids, and they approximate the contribution of a cross-sectional part. By dividing the section into parts, various material characteristics can be assigned to them, which is crucial for analyzing fire and post-fire bearing capacity. Once the interaction surfaces are formulated, the procedure of evaluating utilization of sections is explained based on the inputted sectional forces. The study compares the experimental and numerical results. The findings obtained utilizing this methodology demonstrate good conformity with outcomes obtained through both experimental data and finite element analysis. The investigation illustrates that fire exposure duration has the most substantial influence on compression and bending load-bearing capacity, particularly when subjected to small eccentricity.

Keywords:

fire safety analysis, post-fire analysis, interaction surfaces, ISO 834, Minkowski sum

1 Introduction

To analyze the behavior of structural elements in fire and post-fire scenarios, it is necessary to conduct both thermal and mechanical analyses. Concrete elements exhibit varying degrees of heating due to their size and thermal properties, and some sections have established isotherms for standard fires. However, for other sections, more sophisticated thermal analysis using finite element methods is required to determine reduced material characteristics, followed by mechanical analysis. Accurately accounting for temperature variations within the section demands complex calculations, which can be achieved through simplified approaches or suitable software.

This paper proposes a methodology utilizing the Minkowski sum of ellipsoids to analyze reduced load-bearing capacity in fire and post-fire scenarios. The study includes both thermal and mechanical analyses, and the results are compared to experimental findings.

The approach presented in this paper can subsequently be incorporated into the development of finite elements of point plasticity, enabling the analysis of complex frame

[*] corresponding author: bursacmilan4@gmail.com

structures. This involves approximating beams and columns with 1D finite elements, significantly reducing the computation time of a structure in comparison to what is required for 3D finite element analysis.

2 Formulation of interaction surface based on Minkowski sum of ellipsoids

Using plasticity theory and assuming full cross-sectional plastification, an interaction surface is formulated. The complex geometry of this surface is closely approximated through the Minkowski sum of ellipsoids [1]. To evaluate the bearing capacity of the cross-section, it is divided into segments, and a single ellipsoid is used for each segment (as shown in Figure 1). The ellipsoids depicted in the figure have been scaled up by different factors for improved visibility.

To create ellipsoids, points on their surface corresponding to the cross-sectional bearing capacity must be determined. This requires calculating the bearing capacity for a specific set of failure mechanisms that are defined by the position of the neutral axis. These failure mechanisms take the following form [2] [3] [4] [5]:

$$n = \begin{bmatrix} \dot{\epsilon} \\ \dot{\chi}_2 \\ \dot{\chi}_3 \end{bmatrix} \tag{1}$$

Where:
$\dot{\epsilon}$ – axial strain
$\dot{\chi}_2$ – curvature around axis 2
$\dot{\chi}_3$ – curvature around axis 3
With the condition:

$$\sqrt{\dot{\epsilon}^2 + \dot{\chi}_2{}^2 + \dot{\chi}_3{}^2} = 1 \tag{2}$$

Equation of neutral axis can be written for a chosen mechanism:

$$\dot{\epsilon} + x_3\dot{\chi}_2 - x_2\dot{\chi}_3 = 0 \tag{3}$$

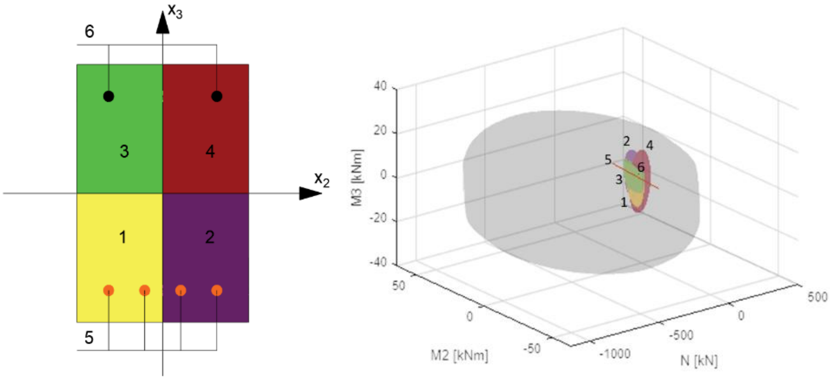

Figure 1: Construction of interaction surface by sum of ellipsoids

Contribution of a single concrete part of the section for the chosen mechanism can be determined:

$$\tau_{yI}[n_k] = \begin{bmatrix} -f_c\Omega_{cI} \\ -f_c \int_{\Omega_{cI}} x_3 \, d\Omega_{cI} \\ f_c \int_{\Omega_{cI}} x_2 \, d\Omega_{cI} \end{bmatrix} \tag{4}$$

Where:

f_c – compressive strength of concrete

Ω_{cI} – compressed surface of cross-sectional part

The compressed portion of the analyzed cross-sectional part is represented by Ω_{cI}, as illustrated in Figure 2. To analyze a concrete beam cross-section using plasticity theory, it is necessary to reduce the compressive strength of the concrete. This reduction is achieved using a procedure outlined in SRPS EN 1994-1-1 [6]. In MATLAB, the integration necessary to evaluate the compressed surface can be accomplished by identifying the compressed nodes of the part and performing integration accordingly.

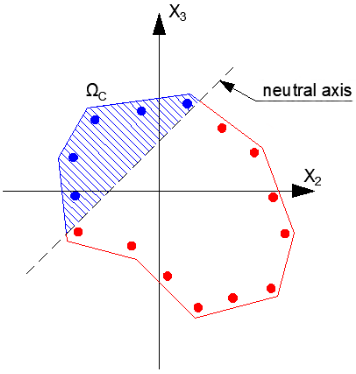

Figure 2: Calculational section for known mechanism

Bearing capacity contribution of a group of rebars is evaluated for chosen mechanism:

$$\tau_{yI}[n_k] = \begin{bmatrix} f_y \sum_{i=1}^{N_{sI}} a_i A_i \\ f_y \sum_{i=1}^{N_{sI}} a_i x_{3i} A_i \\ -f_y \sum_{i=1}^{N_{sI}} a_i x_{2i} A_i \end{bmatrix} \tag{5}$$

With:

$$a_i = sign(\dot{\epsilon} + x_3 \dot{\chi}_{2i} - x_2 \dot{\chi}_{3i}) \tag{6}$$

Where:

f_y – yield strength of steel

A – rebar area

Forming an ellipsoid, for all mechanisms, for a part of the cross section can be done in matrix form [7]:

$$(\tau_I - c_I)^T C_I^{-1} (\tau_I - c_I) = 1 \tag{7}$$

Where c_I is the center of the ellipsoid in following form:

$$c_I = \begin{bmatrix} c_{I1} \\ c_{I2} \\ c_{I3} \end{bmatrix} \tag{8}$$

Shape matrix is decomposed by Cholsky factorization into two matrices:

$$C_I = L_I^{-1} L_I \tag{9}$$

Where:

$$L_I = \begin{bmatrix} y_{I1} & y_{I2} & y_{I3} \\ 0 & y_{I4} & y_{I5} \\ 0 & 0 & y_{I6} \end{bmatrix} \tag{10}$$

The method of least squares is employed to continuously estimate the bearing capacity of individual parts, which has only been evaluated at discrete points corresponding to selected failure mechanisms:

$$min_{(c_I,C_I)} \sum_k r_k^2 \tag{11}$$

Where:

$$r_k = n_k^T(\tau_{yI}[n_k] - \tau_I[n_k]) \tag{12}$$

$$\tau_I[n_k] = c_I + \frac{C_I n_k}{\sqrt{n_k^T C_I n_k}} \tag{13}$$

The fmincon command in MATLAB can be used to easily execute this procedure.

Minkowski sum of ellipsoids can be formulated as a sum of parts load-bearing capacity:

$$\tau[n] = \sum_I \tau_I[n] \tag{14}$$

Where:

$$\tau_I[n_k] = c_I + \frac{C_I n}{\sqrt{n^T C_I n}} \tag{15}$$

2.1 Transformation of interaction surface for fire situation

Ellipsoids for the cross-sectional parts are created only once for the temperature condition prior to the occurrence of fire. To account for the transformation of the interaction surface, each ellipsoid is scaled by reduction coefficients listed in section 3, based on the average temperature in each part of the cross-section using the following expression:

$$\tau[n,t] = \sum_I \bar{k}_I[t]\tau_I[n] \tag{16}$$

Where:

$\bar{k}$ – reduction coefficient based on parts average temperature

2.2 Cross-sectional utilization evaluation

The internal forces of the analyzed cross-section can be expressed in vector form:

$$\tau^* = \begin{bmatrix} N \\ M_2 \\ M_3 \end{bmatrix} \tag{17}$$

Where:

N – axial force

M_2 – bending moment around axis 2

M_3 – bending moment around axis 3

To determine the cross-sectional utilization for a given set of internal forces, a system of equations must be constructed using the algorithm outlined in Figure 3 [8] [9] [10].

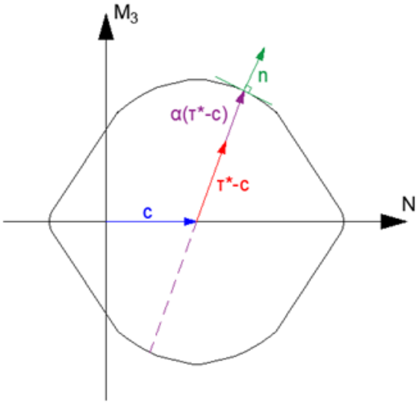

Figure 3: The algorithm used to determine the cross-sectional utilization

Figure 3 illustrates the interaction diagram for normal force and bending moment around a single axis, with the central point represented by vector c. Subtracting vector c from the internal forces vector τ^* yields a new vector that originates from the center of the diagram and can be utilized to assess the cross-sectional utilization.

Section of the line that is colinear with vector $\tau^* - c[t]$ and the interaction surface can be written in following way:

$$r_n = \tau[n,t] - c[t] - \alpha(\tau^* - c[t]) = \sum_I \left(\bar{k}_I[t]\frac{C_I n}{\sqrt{n^T C_I n}}\right) - \alpha(\tau^* - c[t]) = 0 \tag{18}$$

Where:

$$c[t] = \sum_I \bar{k}_I[t] c_I \tag{19}$$

The coefficient α represents the cross-sectional utilization and indicates the scaling factor needed for the intensity of the vector $\tau^* - c[t]$ to come into contact with the interaction surface.

A total of three equations with four unknowns are formed, thus an additional equation is required to solve the problem. The following normalization can be used due to the convexity of the interaction surface:

$$r_\alpha = 1 - n^T(\tau^* - c[t]) = 0 \tag{20}$$

With the previous procedure the problem of two solutions is avoided and the required solution can be evaluated.

Nonlinear system of equations $r = \{r_n{}^T, r_\alpha\}^T$ with unknowns $z = \{n^T, \alpha\}^T$ can be solved by fsolve command in MATLAB.

3 Material characteristics in fire and post-fire situation

3.1 Thermal material characteristics in fire situation

Required parameters for thermal analysis are: specific heat, thermal conductivity and the change in material density in fire situation.

Those characteristics can be found for concrete in SRPS EN 1992-1-2 [11] and for steel in SRPS EN 1993-1-2 [12].

3.2 Mechanical material characteristics in fire situation

Mechanical material characteristics in elevated temperatures decrease. Dependence of temperature and reduction intensity of material characteristics is provided in standards and evaluated experimentally. Chosen standard for reduction of material characteristics in this paper is SRPS EN 1992-1-2.

3.3 Mechanical material characteristics in post-fire situation

Experimental data suggests that the material characteristics do not fully return to their initial state after a fire. These remaining characteristics, known as residual characteristics, depend on the maximum temperature experienced by the cross-section during the fire. Over time, the residual characteristics of concrete improve. For that reason, the analysis is performed immediately after the fire has been extinguished. The relationship between the residual characteristics and the temperature of the cross-section is provided in Annex C of Eurocode 1994-1-2 [13].

The paper [14] examines the characteristics of rebar steel after being exposed to fire. The dependence between the residual characteristics and the maximum temperature θ_{max} in a fire situation is established based on experimental results:

$$f_{y,\theta,20°C} = \varphi f_y \tag{21}$$

Reductional coefficient φ can be determined based on cross-sectional temperature with following expressions:

$$\varphi = 1 \qquad 20°C \leq \theta_{max} < 500°C \tag{23}$$

$$\varphi = 1.5 - \frac{\theta_{max}}{1000} \qquad 500°C \leq \theta_{max} < 800°C \tag{24}$$

$$\varphi = 0.7 \qquad \theta_{max} \geq 800°C \tag{25}$$

4 Analysed problem

The beam shown in Figure 4 is analyzed in [15] using Abaqus, while its experimental analysis is presented in [16]. This paper presents a thermal and mechanical analysis of the same beam and compares the results with those obtained in the experiment.

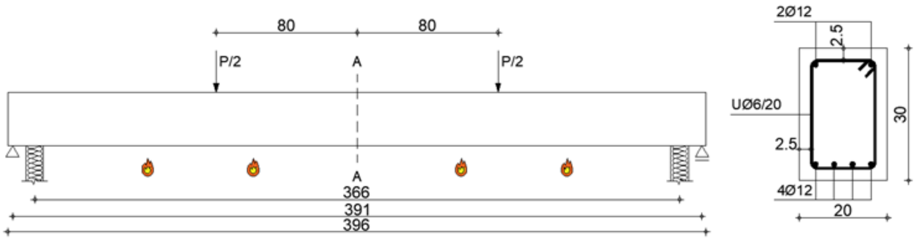

Figure 4: Analyzed beam

Beam has rectangular cross section with dimensions of 200 x 300 mm. Lower zone is reinforced with 4Φ12, while upper with 2Φ12. Adopted stirrups are Φ6/20 cm. Concrete cover is 25 mm thick. The compressional strength of the concrete is 17 MPa, while the yield strength of the steel is 415 MPa. Beams span is 3910 mm. Analyzed beam is loaded with two concentrated forces with intermediate distance of 1600 mm to accomplish constant bending moment and more accurate measurement. After determined fire exposure, beam is loaded until fracture occurs.

5 Thermal analysis

A thermal analysis is conducted based on the ISO 834 standard fire. Analysis was performed in Transient Thermal subprogram of ANSYS Workbench with required material parameters as defined in section 3. The temperature curve for the gas in the room engulfed in fire is provided in SRPS EN 1991-1-2 [17]. The heat from the gas is transferred to the structure through convection and radiation. According to [17], the coefficient of convection for sides directly exposed to the fire can be assumed to be 25 W/m^{2}K, while the coefficient for sides not directly exposed to the fire takes into account both convection and radiation, and its recommended value is 9 W/m^{2}K. The intensity of radiation on the element's sides, that are directly exposed to fire, is determined by the surface emissivity coefficient, which has a value of 0.8. The concrete's assumed humidity is 1.5%.

The beam specified in section 4 is subjected to direct fire from the sides and from below. The temperature profiles are computed for fire durations of 60, 90, and 120 minutes. The resulting temperature profiles are illustrated in Figures 5, 6, and 7.

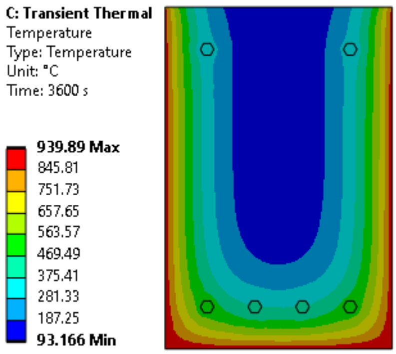

Figure 5: Beams temperature profile for 60 min. of standard fire

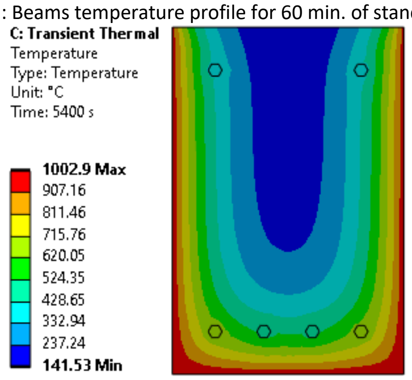

Figure 6: Beams temperature profile for 90 min. of standard fire

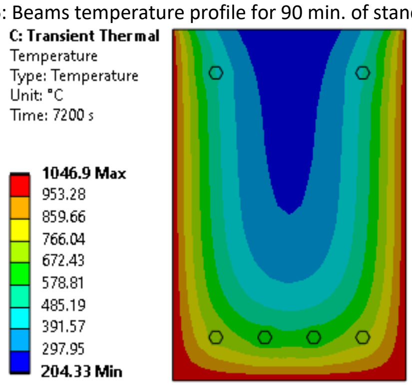

Figure 7: Beams temperature profile for 120 min. of standard fire

6 Mechanical analysis

The mechanical analysis is conducted based on the thermal analysis and theoretical principles presented in section 2. To achieve a more precise interaction surface and temperature changes in the cross section, the concrete component of the cross section is divided into 16 sections, each described by a distinct ellipsoid. The rebars are combined into two ellipsoids. The cross-sectional discretization is illustrated in figure 8.

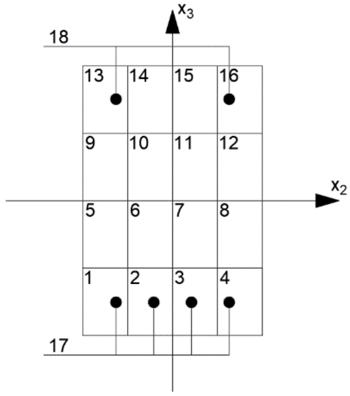

Figure 8: Discretization of the cross section

The computed outcomes are compared with the experimental data measured in [16], outcomes obtained by the simplified calculation model presented in [15], and results determined by the finite element method in [18]. Some of the papers present their findings in terms of the maximum applied force, while others report the maximum moment caused by the force. To facilitate comparison, all results have been presented in terms of bending moment. Table 1 displays the results.

Table 1: Comparison of calculated and measured results

Time	Residual bearing capacity [kNm]			
	Measured [16]	**Kodur et al. [18]**	**Kodur et al. [15]**	**Calculated**
t = 0	54.25	54.87	48.99	51.41
t = 60 min.	46.50	46.20	42.50	43.93
t = 90 min.	39.30	40.01	39.10	37.92
t = 120 min.	30.73	34.13	29.49	33.26

In Figure 9a), it is possible to compare the interaction surfaces for residual bearing capacity and observe their reduction for various lengths of fire exposure. Additionally, Figures 9b), c), and d) feature interaction diagrams, which offer a better possibility of reduction observation. However, these diagrams only consist of two internal forces, and the value of the third internal force, which is not included in the diagram, is zero.

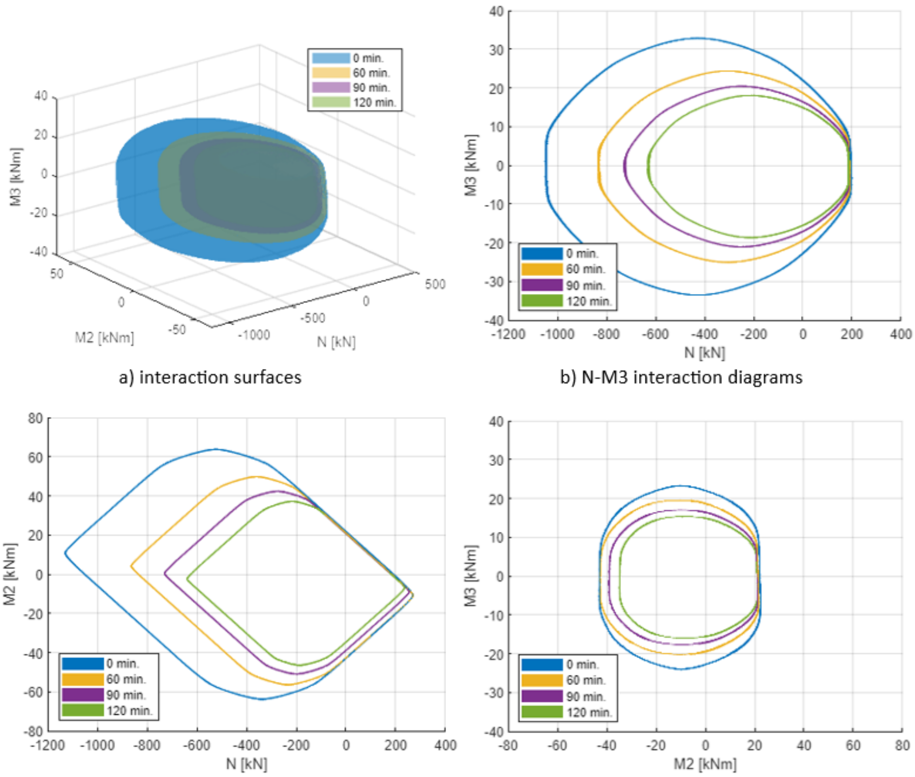

a) interaction surfaces b) N-M3 interaction diagrams

c) N-M2 interaction diagrams d) M2-M3 interaction diagrams

Figure 9: Comparison of interaction surfaces and diagrams for different fire durations

7 Conclusion

The method presented involves calculating the bearing capacity of each cross-sectional part and scaling it based on the reduction coefficient calculated from the average temperature of that part. The cross-sectional bearing capacity is then determined by summing the bearing capacity contributions from all the parts.

The results obtained through this method show good agreement with values obtained using the finite element method and experimental results. Discrepancies in the results presented in Table 1 arise from the simplification of the actual stress state in the cross-section, which assumes uniform pressure in the compressed region. This simplification is employed in both the present paper and the calculation presented in reference [15], accounting for the highest level of similarity between their respective outcomes. Conversely, more sophisticated analysis utilizing 3D finite elements, which does not employ this simplification, generates results that are in better agreement with experimental findings but is considerably more computationally intensive.

The analysis reveals that the effect of fire exposure length has the greatest impact on compression and bending with small eccentricity load-bearing capacity. This is due to a greater reduction in the residual strength of concrete compared to steel.

References

[1] Y. Yan and G. S. Chirikjian, “Closed-form characterization of the Minkowski sum and difference of the two ellipsoids,” *Springer,* 2014.

[2] J. Blayer and P. de Buhan, “Yield surface approximation for lower and upper bound yield design of 3D composite frame structures,” *Computers and Structures,* 2013.

[3] D. T. Pham, P. de Buhan, C. Florence, J.-V. Heck and H. H. Nguyen, “Interaction diagrams of reinforced concrete sections in fire: A yield design approach,” *Engineering Structures,* 2015.

[4] L. Leonetti, R. Casciaro and G. Garcea, “Effective treatment of complex statical and dynamical load combinations within shakedown analysis of 3D frames,” *Computers and Structures,* 2015.

[5] S. Sessa, F. Marmo, L. Rosati, L. Leonetti, G. Garcea and R. Casciaro, “Evaluation od the capacity surfaces of reinforced concrete sections: Eurocode versus a plasticity-based approach,” *Springer,* 2017.

[6] SRPS EN 1994-1-1 Еврокод 4 – Пројектовање спрегнутих конструкција од челика и бетона – Део 1-1: Општа правила и правила за зграде, Институт за стандардизацију Србије, 2012.

[7] D. Magisano, F. Liguori, L. Leonetti and G. Garcea, “Minkowski plasticity in 3D frames: Decoupled construction of the cross-section yield surface and efficient stress update strategy,” *John Wiley & Sons Ltd.,* 2018.

[8] D. Magisano, F. Liguori, L. Leonetti, D. de Gregorio, G. Zuccaro and G. Garcea, “A quasi-static nonlinear analysis for assessing the fire resistance of reinforced concrete 3D frames exploiting time-dependent yield surfaces,” *Computers and Structures,* 2018.

[9] W. M. Coombs, O. A. Petit and Y. G. Motlagh, “NURBS plasticity: yield surface representation and implicit stress integration for isotropic inelasticity,” *Computer methods in applied mechanics and engineering,* 2016.

[10] W. M. Coombs and Y. G. Motlagh, “NURBS plasticity: non-associated plastic flow,” *Computer methods in applied mechanics and engineering,* 2018.

[11] SRPS EN 1992-1-2 Eurocode 2 – Design of concrete structures – Part 1-2: General rules – Structural fire design, Institute for standardization of Serbia, 2012.

[12] SRPS EN 1993-1-2 Eurocode 3 – Design of steel structures – Part 1-2: General rules – Structural fire design,, Institute for standardization of Serbia, 2012.

[13] SRPS EN 1994-1-2 Eurocode 4 – Design of composite steel and concrete structures – Part 1-2: General rules – Structural fire design, Institute for standardization of Serbia, 2012.

[14] I. Neves, J. P. C. Rodriques and A. D. P. Loureiro, “Mechanical properties of reinforcing and prestressing steels after heating,” *Journal of Materials in Civil Engineering,* 1996.

[15] V. K. R. Kodur, M. B. Dwaikat and R. S. Fike, “An approach for evaluationg the residual strength of fire-exposed RC beams,” *Magazine of Concrete Research,* 2010.

[16] A. Kumar and V. Kumar, “Behaviour of RCC beams after exposure to elevated temperatures,” *Journal of The Institution of Engineers (India),* 2003.

[17] SRPS EN 1991-1-2 Eurocode 1 – Action on structures – Part 1-2: General actioins – Action on structures exposed to fire, Institute for standardization of Serbia, 2012.

[18] V. K. R. Kodur and A. Agrawal, “An approach for evaluationg residual capacity of reinforced concrete beams exposed to fire,” *Engineering structures,* 2015.